Ultrafast X-Ray Absorption Spectroscopy of Strongly Correlated Systems: Core Hole Effect

Chen-Yen Lai and Jian-Xin Zhu

Phys. Rev. Lett. **122**, 207401 — Published 22 May 2019

DOI: 10.1103/PhysRevLett.122.207401

Ultrafast x-ray absorption spectroscopy of strongly correlated systems: Core hole effect

Chen-Yen Lai and Jian-Xin Zhu
Theoretical Division, Los Alamos National Laboratory, Los Alamos, New Mexico 87545, USA and
Center for Integrated Nanotechnologies, Los Alamos National Laboratory, Los Alamos, New Mexico 87545, USA
(Dated: April 29, 2019)

In recent years, ultrafast pump-probe spectroscopy has provided insightful information about non-equilibrium dynamics of excitations in materials. In a typical experiment of time-resolved x-ray absorption spectroscopy, the systems are excited by a femtosecond laser pulse (pump pulse) following by an x-ray (probe pulse) after a time delay to measure the absorption spectra of the photoexcited systems. We present a theory for nonequilibrium x-ray absorption spectroscopy in one-dimensional strongly correlated systems. The core hole created by x-ray is modeled as an additional effective potential on the core hole site which changes the spectrum qualitatively. In equilibrium, the spectrum reveals the charge gap at half-filling and the metal-insulator transition in the presence of core hole effect. Furthermore, a pump-probe scheme is introduced to drive the system out of equilibrium before the x-ray probe. Effects of the pump pulse with varying frequency, shape and fluence are discussed on the dynamics of strongly correlated systems for in and out of resonance. The spectrum indicates that the driven insulating state has a metallic droplet around the core hole. The rich structures of nonequilibrium x-ray absorption spectrum give more insight on the dynamics of electronic structures.

The primary goal of x-ray spectroscopy is to probe the properties of core level electrons and its coupling to the electrons near Fermi energy [1, 2]. In contrary to the angle-resolved photoemission spectroscopy, which provides an accurate measurement of low-energy band structure [3–6], the x-ray spectroscopy offers a sensitive and versatile probe of the high-energy excitations. On the other hand, the rapidly developed resonant inelastic x-ray scattering, a photon-in photon-out process, provides more information on the excitation spectrum [7–10]. The short time evolution of slightly excited initial state in both bosonic and fermionic systems can be exploited to answer fundamental questions in condensed matter physics and strongly correlated systems. In cold atom systems where the atoms have relatively slow motions [11], several studies have investigated the relaxation of the quantum state after the sudden quench [12, 13] and proposed scheme to probe the properties of many-body state [14–16]. The ultrafast laser spectroscopy provides an additional gear to investigate the electronic structure of excited states in materials. Although the photoexcited carriers usually have short lifetime [17], the state-of-the-art pump-probe technique can still study the time evolution of the materials, for instance, cuprate superconductors [9, 18, 19], transition metal oxides [20, 21], and charge density wave compounds [19, 22–24]. Along with the development of table-top x-ray source [25, 26], the reconstruction of the charge, spin, and lattice dynamics [27, 28] from time-resolved x-ray spectroscopy is within reach. The obtained insight will be very helpful in understanding emergent phenomena in strongly correlated electron systems, among which Mott insulator-metal transition is one of the intriguing phenomena and the properties of excited state spectrum is difficult to measure. By using x-ray absorption in experiments [29–31], one can determine the metal-insulator transition as the temperature varies or doping changes [18]. The dynamics of such systems, driven out of equilibrium by external stimuli, can provide insight into the underlying interactions between different coupling mechanisms within femto to picosecond time scales [32, 33]. Selective measurement techniques are necessary to probe specific excitations since the connection between various types of excitations is hidden deep in the quantum wavefunction, which cannot be observed directly.

Different from other probe techniques, the x-ray absorption spectroscopy (XAS) also brings out the core hole effect [34–37]. Combined with the valance-electron quantum dynamics, the core hole effect is expected to create novel phenomena in non-equilibrium systems. In this Letter, we propose a single band model to study both the static and nonequilibrium (NE) XAS of one-dimensional strongly correlated systems. We model the core hole created by the incident x-ray as an attractive potential to the valence electrons [38]. In equilibrium, the spectrum reveals the metal-insulator transition for systems at the half filling due to the core hole effect. The NE spectrum have even more features including a metallic droplet around the core hole from a driven insulating state. Furthermore, the NE-XAS shows a resonance between the frequency of the incidental pump pulse and the charge gap of the systems.

Theoretical formalism – Starting from a conventional two-orbital model [38] and considering the dipole matrix element: $\langle 3d_\sigma|T_\sigma|2p\rangle$ between two orbitals for absorption where T_σ is a dipole transition operator, we propose an effective single band model to capture the x-ray absorption spectrum. In equilibrium, the valance electron are described by a Fermi-Hubbard model (FHM),

$$\mathcal{H} = -J\sum_{\langle ij\rangle,\sigma}(d^\dagger_{i\sigma}d_{j\sigma} + h.c.) + U\sum_i n_{i\uparrow}n_{i\downarrow}, \qquad (1)$$

where $d^\dagger_{i\sigma}$ is fermion creation operator with spin-σ at site-i and the density operator is $n_{i\sigma} = d^\dagger_{i\sigma}d_{i\sigma}$. Hereafter, the hopping amplitude is set to unity $J = 1$ and time unit is $t_0 = \hbar/J$. In general, the XAS can be determined from the Fermi

Golden rule

$$\mathcal{I}_{\rm XAS}(\omega) = \sum_{\sigma}\sum_{F} |\langle F|d^{\dagger}_{m\sigma}|I\rangle|^2 \delta(E_F - E_I - \hbar\omega). \quad (2)$$

Here, $|I\rangle$ ($|F\rangle$) and $E_{I(F)}$ are the initial (final) states and energies, $d^{\dagger}_{m\sigma}$ denotes the electron excited from core level to valence band with spin σ at site-m. Using the identity $\delta(x) = -\frac{1}{\pi}\lim_{\Gamma\to 0^+}{\rm Im}\left\{\frac{1}{x+i\Gamma}\right\}$, the intensity can be expressed as $\mathcal{I}_{\rm XAS}(\omega) = -\frac{1}{\pi}\sum_{\sigma}{\rm Im}\mathcal{A}_{\sigma}(\omega)$, with the quantity $\mathcal{A}_{\sigma}(\omega)$ given by

$$\begin{aligned}\mathcal{A}_{\sigma}(\omega) &= -i\int_0^{\infty} dt e^{i\omega t}e^{-\Gamma t}\mathcal{A}_{\sigma}(t) \quad (3)\\ &= -i\int_0^{\infty} dt e^{i\omega t}e^{-\Gamma t}\langle I|e^{i\mathcal{H}t}d_{m\sigma}e^{-i\mathcal{H}_m t}d^{\dagger}_{m\sigma}|I\rangle.\end{aligned}$$

Here, the Γ represents the core hole lifetime broadening effect. The $\mathcal{H}_m$ inside the non-local time correlation function $\mathcal{A}(t)$ is the sum of the equilibrium Hamiltonian $\mathcal{H}$ and the effective attractive potential $-V_{\rm ch}\sum_{\sigma} n_{m\sigma}$ due to the presence of core hole. In some of the transition metal oxides, the typical core-valence interaction is about 30% stronger than the valence-valence interaction [38, 39]. The initial state, $|I\rangle$, is the many-body wavefunction right before the x-ray probe kicks in. Below we consider two situations: (i) the initial state is ground state of the Hamiltonian and (ii) a NE initial state encoding the effect of pump pulse.

Static XAS – In the equilibrium case, we use the ground state of Eq. (1) as initial state, which can be obtained by density matrix renormalization group accurately [13, 40, 41]. For non-interacting fermions, the wavefunction is a Slater determinant, which can be expressed as a matrix product state (MPS) [41, 42]. Here, different initial interactions and filling fractions, $\bar{n}_f = \sum_{i\sigma} n_{i\sigma}/L$ where L is the number of lattice sites, are studied. The non-local time correlation function is solved in time evolving block decimation [43–45] under MPS framework [13, 46–49]. Since the initial state is the ground state of the FHM, the evolution operator acting on the *bra* state can be reduced to a phase factor, i.e. $\langle GS|e^{i\mathcal{H}t} = e^{iE_{GS}t}\langle GS|$ with ground state energy E_{GS}. Due to the finite lifetime of the core hole, the simulation of real time dynamics is not required to be long to capture the spectrum quantitatively. Throughout this work, we use time step $\delta t = 10^{-3}t_0$ in second order Suzuki-Trotter approximation for time evolution and core hole lifetime $\Gamma = 0.2J$ for calculations of spectra.

The main objective is to capture the core hole effect in the XAS of strongly correlated systems. Starting from non-interacting Fermi sea state at half filling, shown in Fig. 1(a), the results show that the spectrum is split into two peaks from one due to the core hole potential. It is worthy to mention that the spectrum corresponds to the absorption part of the spectral density in the absence of core hole potential [38]. The locations of the peak indicate the corresponding bound state energy due to core hole potential, which is around ω_d (ω_s) for doubly- (singly)-occupied bound state at the core hole site, as marked in Fig. 1(a) where the amplitudes of both

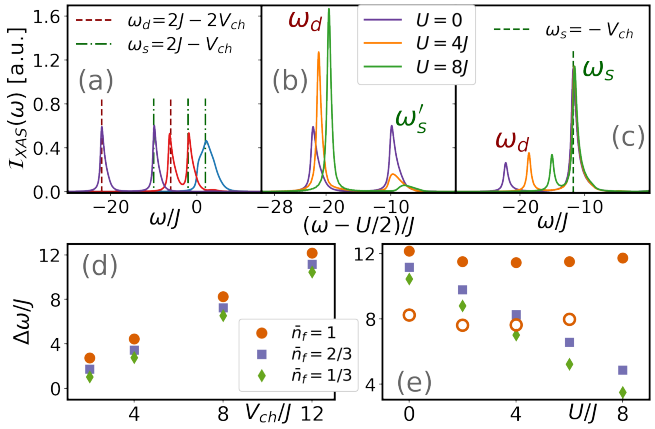

FIG. 1. The static XAS under filling fraction (a)-(b) $\bar{n}_f = 1$ and (c) $\bar{n}_f = 2/3$. In (a), the initial state is Fermi sea state ($U = 0$) and different core hole potentials, $V_{ch}/J = 0$ (blue), 4 (red), 12 (purple), are considered. The spectrum splits in the presence of non-zero core hole potential. In (b) and (c) with shared legend, the initial state is the ground state with different U's and the core hole potential is set to $V_{\rm ch} = 12J$. (d) The frequency difference versus core hole potential from Fermi sea state with different fillings. (e) The frequency difference versus interaction with different fillings where the core hole potential is set to $V_{\rm ch} = 12J$ (filled) and $V_{\rm ch} = 8J$ (open).

peaks are roughly the same. The difference of these two frequencies, $\Delta\omega = \omega_s - \omega_d$, reveals the core hole potential as shown in Fig. 1(d) on all three different fillings. For interacting fermions away from the half filling, shown in Fig. 1(c), the singly-occupied state still has stronger amplitude and all peaks around $-V_{\rm ch}$, which signals the presence of core hole potential. On the other hand, the doubly-occupied state shifts in frequency as the interaction changes and is around $U - 2V_{\rm ch}$. This explains the energy difference $\Delta\omega = V_{\rm ch} - U$ as shown in the Fig. 1(e). Therefore, the XAS can enable us to determine the core hole potential and the interacting strength of the measured strongly correlated systems. For systems at half filling, three different interaction strength are compared in Fig. 1(b). In order to make a comparison to free fermions, the frequency is shifted to match the symmetric point determined by the density of states [38]. Comparing to the systems away from half filling, where only the doubly-occupied state has the frequency shifted by U, both peaks are now shifted due to the strongly correlated effects. After the core electron is excited, the core hole site is nearly a doubly-occupied in this Mott insulating phase. Since the filling factor is exactly at half originally, the excess electron forms a doublon even if the electron escapes from the core hole site. This doublon outside the core hole site makes the frequency of singly-occupied bound state shifted by U as well as the doubly-occupied bound state. Therefore, in the half filling, the energy of singly-occupied state is shifted to $\omega'_s = U - V_{\rm ch}$ and the frequency difference is independent of the interaction as two different core hole potentials shown in Fig. 1(e).

In addition, the weight of corresponding response also re-

veals important information about electronic structure. It is defined as

$$\mathcal{W}_i = \int_{\omega_i-\delta\omega}^{\omega_i+\delta\omega} \mathcal{I}_{\rm XAS}(\omega)d\omega, \tag{4}$$

where the $\delta\omega$ is a finite width that covers the decay tail due to the broadening. The spectrum is normalized such that $\sum_i \mathcal{W}_i \approx 2$ due to spin degrees of freedom. It is known that the charge gap exists in one-dimensional half-filled FHM with any finite U in the thermodynamic limit [50, 51]. From Fig. 1(b), we can immediately observe this feature. In the absence of interaction, both singly- and doubly-occupied bound state have almost the same weight. As the interaction increases, the weight of doubly-occupied state *always* dominates over the singly-occupied state. We notice that the chemical potential shift is not only manifesting in the change of the dominant peak position, but also the relative intensity transfer between the ω_d and ω_s peaks [52, 53]. Also, this weight transfer depends on the strength of both Hubbard interaction and the core hole potential. Figures 2(b) and (c) give a more quantitatively analysis on the shifting weight for varying interaction strength and core hole potential. At the half filling, both peaks have equal weight from the Fermi sea state and the signals from doubly-occupied state becomes more dominant as the interaction becomes finite for various core hole potentials, especially in a deep core hole potential (compare the weight for $V_{\rm ch} = 4J$ and $8J$ in Fig. 2(b)). This suggests that the charge gap opens in finite interactions. In the low electron occupation limit, the dominant signals is always the singly-occupied state as shown in Fig. 2(c). In the weak interaction regime, $U < 4J$, the weight distributions are almost identical despite different core hole potentials.

Nonequilibrium XAS – When a laser pulse is incident before the x-ray photon, the initial state in Eq. (3) is no longer the ground state of the FHM. We model the effect of the laser pulse via a time-dependent *Pieles* phase in the Hamiltonian, $J \to Je^{iA(t)}$, where the phase has a gaussian profile, $A(t) = A_0 e^{-(t+t_d)^2/2\tau^2}\cos\Omega(t+t_d)$ with intensity A_0, central frequency Ω and pulse shape with width τ and a time delay t_d (We set the probe always starting at $t = 0$). The average incoming number of photons per lattice site from the pump is

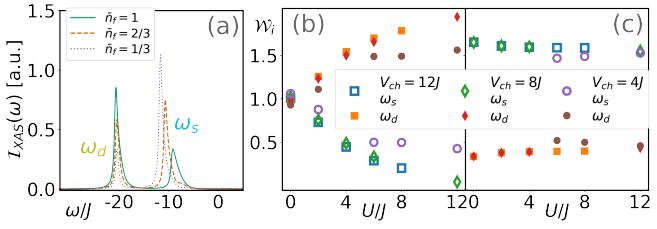

FIG. 2. (a) The XAS for different fillings under the same interaction $U = 2J$ and core hole potential $V_{\rm ch} = 12J$. The weight of XAS from singly (open symbols) and doubly (fille symbols) occupied state in (b) $\bar{n}_f = 1$ and (c) $\bar{n}_f = 1/3$ under different interactions and core hole potentials.

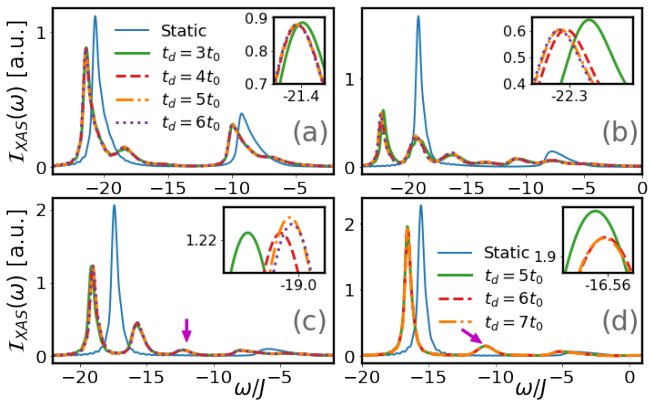

FIG. 3. The NE-XAS with core hole potential $V_{\rm ch} = 12J$ and different time delay for (a) $U = 2J$, (b) $4J$, (c) $6J$, and (d) $8J$ under the pulse fluence $\Omega t_0 = 3$, $\tau = 2t_0$, $A_0 = 0.1$ in (a)-(c), and $A_0 = 0.3$ in (d). In (c) and (d), the peak around $\omega \sim -12J$ (magenta arrow) emerges as a singly-occupied core hole signal from the metallic droplet. The system is at the half filling.

estimated to be $\propto A_0^2\Omega\tau$. In order to capture the effect from the pump pulse, the time delay is chosen large enough where the amplitude of the pulse is almost vanished ($A(0) < 0.1$) before measuring the XAS. Therefore, the real time dynamics of initial ground state wavefunction under the pulse needs to be simulated before calculating the non-local time correlation function. In other words, the initial state in Eq. (3) is given by $|I\rangle = \hat{U}(-2t_d, 0)|GS\rangle$, where $\hat{U}$ is the time evolution operator of the FHM including the interaction with the electromagnetic field.

We first vary only the time delay by keeping the pulse intensity, frequency, and shape fixed. The NE-XAS for the half filling is shown in Fig. 3 with different time delay t_d. Since our model does not include the relaxation effect, the NE-XAS will *never* recover back to the equilibrium one even after an extended time delay. Here, the spectrum from different time delays does not change much since the state only picks up some extra phases after the tail of the pulse diminishes. Small changes of the frequency and amplitude (See the insets of Fig. 3) are due to the infinitesimal tail of the pulse. As long as the time delay is long enough, the signals become translational invariant in time as one compares the $t_d = 5t_0$ and $6t_0$. Also, the shifting of the peaks is roughly equal to the energy changes of the state from the pumping. Beside that, the spectrum is qualitatively different from the one at equilibrium. First of all, there are only two major peaks in the equilibrium spectrum, but the NE-XAS exhibits much rich feature from the excited states. For the weak interaction case, e.g. $U = 2J$, new peaks emerge around $\omega_{d(s)} + 3J$, where the shift matches the pump pulse frequency Ω. As the interaction increases to $4J$, the fluence from the pulse is severe and this is because the Mott gap is close to the frequency of the pump pulse. This resonance effect will be elaborated later. Once the interaction reaches $6J$ and $8J$, a new peak emerges around $-V_{\rm ch}$. As we

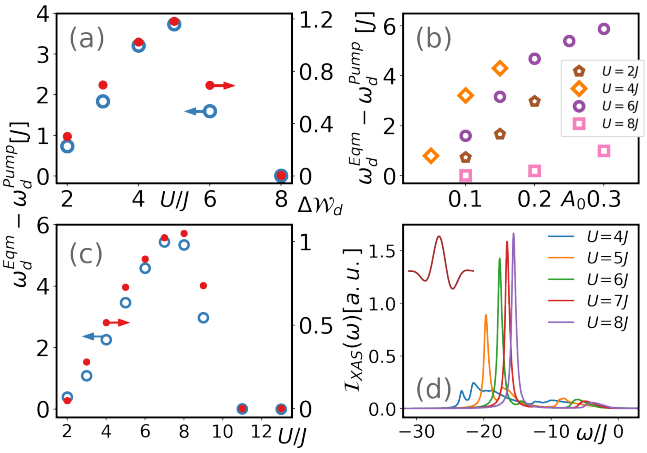

FIG. 4. (a) The changes of weight (filled symbols) and frequency (empty symbols) of the doubly occupied state versus interaction under the intensity $A_0 = 0.1$. (b) The frequency shift of the doubly occupied state versus different intensity under different interactions. In (a) and (b), the pump pulses have $\Omega t_0 = 3$, $\tau = 2t_0$, and $t_d = 6t_0$. (c) The changes of weight (filled symbols) and frequency (empty symbols) of the doubly occupied state versus interaction when systems at half filling under fluence $\Omega t_0 = 6$, width $\tau = 3t_0$, time delay $t_d = 6t_0$, and $A_0 = 0.1$. (d) The NE-XAS for systems at half filling with different U's under single cycle THz pulse fluence $\Omega t_0 = 1$, width $\tau = 3t_0$, time delay $t_d = 6t_0$ and intensity $A_0 = 1$. The inset shows the THz pulse profile. The core hole potential is set to $V_{\rm ch} = 12J$ in all panels.

have discussed in the equilibrium spectrum, this energy corresponds to the singly-occupied state (ω_s) from a metallic state. Since the photoemission spectrum shows that the system remains gapped [38], the results conjecture that this metallic signal is induced by the core hole and should be a droplet around the core hole site. The similar effect is reported in superconductors with impurity or disorder [54].

We then vary the intensity of pulse to study the quantitative change of the NE-XAS, by using the same time delay $t_d = 6t_0$ to ensure the pump pulse is almost finished. In Fig. 4, quantitative analysis of nonequilibrium XAS are shown under different shapes of the pump pulse. For all interaction strengths, both the singly- and doubly-occupied peaks get smaller weight as the intensity increases. One expects that the system will melt down and the spectrum will become complete featureless as the state is excited into the continuum when the pump pulse is very strong. Before that, the spectrum appear to have peaks separated by the energy closed to pump pulse frequency. More interestingly, the pump pulse used here has frequency $\Omega t_0 = 3$ and strongest influence on the $U = 5J$ state. Considering the same intensity, $A_0 = 0.1$ and 0.15 for example, the shift of frequency of the doubly-occupied state are larger for $U = 5J$ as shown in Fig. 4(b). As the interaction increases to $6J$ and $8J$, the effects of frequency shift and the weight of doubly-occupied state are also smaller than the one of $U = 5J$, where the detail comparison is shown in Fig. 4(a). By switching the frequency to $\Omega t_0 = 6$, the detail spectrum is shown in Supplemental Material and the shifting of frequency is shown in Fig. 4(c). The shift of frequency is bigger as the interaction increases and reaches maximum around $8J$. The effect diminishes once the interaction becomes stronger. From the results of two different frequencies, both the shift of frequency and the change in the weight of the doubly-occupied state give the same conclusion that there is a resonance between the pump pulse frequency and the the charge gap in the systems. On the other hand, for the single cycle terahertz (THz) pulse with frequency $\Omega t_0 = 1$, as shown in Fig. 4(d), the results show that the spectrum becomes featureless for weak and intermediate interactions (e.g. $U \leq 4J$). As the interaction becomes stronger, the NE-XAS is less affected by the pump pulse. For instance, $U = 8J$, the shift of frequency and change in weight are minimal when compared to the static XAS.

Conclusion – We have proposed a single band model to capture the core hole effect in the XAS and calculated the spectrum of one-dimensional strongly correlated system. The static XAS is able to distinguish the corresponding core hole potential and interaction strength of the strongly correlated materials. Due to the strongly correlated effect, the static XAS reveals the charge gap from the doubly-occupied bound state when the system is half filling with finite interaction. Furthermore, considering the pump pulse with different time delay, intensity and frequency, the NE-XAS show that the driven system has a metallic droplet around the core hole, which is a similar phenomenon as an impurities influence the electronic states of superconductors. Our results have uncovered that the static and nonequilibrium XAS can help to identify the excitations contributing to the spectrum and guide the future pump-probe experiments on strongly correlated materials, such as $Sr_2CuO_{3+\delta}$ [55–57] or other cuprate compounds with Cu-O corner (or edge) sharing chains [57–59]. Those materials can be successfully synthesized and some of them can be doped away from the half filling, on which the photoemission spectrum have also been measured [55].

We thank Jhi-Shih You and Marton Kanász-Nagy for fruitful discussion in the early stage of this work. This work was carried out under the auspices of the U.S. Department of Energy (DOE) National Nuclear Security Administration under Contract No. 89233218CNA000001. It was supported by the Center for Integrated Nanotechnologies, a DOE Office of Science User Facility, and in part by the LANL LDRD Program. The numerical programs were built upon universal tensor library [60] and the computational resource was provided by the LANL Institutional Computing Program.

[1] L. J. P. Ament, M. van Veenendaal, T. P. Devereaux, J. P. Hill, and J. van den Brink, Rev. Mod. Phys. **83**, 705 (2011).
[2] W. Olovsson, L. Weinhardt, O. Fuchs, I. Tanaka, P. Puschnig, E. Umbach, C. Heske, and C. Draxl, J. Phys.: Condens. Matter **25**, 315501 (2013).
[3] A. Damascelli, Z. Hussain, and Z.-X. Shen, Rev. Mod. Phys. **75**, 473 (2003).

[4] J.-X. Zhu, A. V. Balatsky, T. P. Devereaux, Q. Si, J. Lee, K. McElroy, and J. C. Davis, Phys. Rev. B **73**, 014511 (2006).
[5] A. A. Kordyuk, Low Temp. Phys. **40**, 286 (2014).
[6] A. Avella and F. Mancini, eds., *Strongly Correlated Systems*, Experimental Techniques (Springer-Verlag, Berlin Heidelberg, 2015).
[7] L. J. P. Ament, G. Khaliullin, and J. van den Brink, Phys. Rev. B **84**, 020403(R) (2011).
[8] M. P. M. Dean, Y. Cao, X. Liu, S. Wall, D. Zhu, R. Mankowsky, V. Thampy, X. M. Chen, J. G. Vale, D. Casa, et al., Nat. Mater. **15**, 601 (2016).
[9] H. Y. Huang, C. J. Jia, Z. Y. Chen, K. Wohlfeld, B. Moritz, T. P. Devereaux, W. B. Wu, J. Okamoto, W. S. Lee, M. Hashimoto, et al., Sci. Rep. **6**, 19657 (2016).
[10] M. Minola, G. Dellea, H. Gretarsson, Y. Y. Peng, Y. Lu, J. Porras, T. Loew, F. Yakhou, N. B. Brookes, Y. B. Huang, et al., Phys. Rev. Lett. **114**, 217003 (2015).
[11] C.-C. Chien, S. Peotta, and M. Di Ventra, Nat. Phys. **11**, 998 (2015).
[12] C.-Y. Lai and C.-C. Chien, Phys. Rev. Applied **5**, 034001 (2016).
[13] C.-Y. Lai and C.-C. Chien, Phys. Rev. A **96**, 033628 (2017).
[14] R. Senaratne, S. V. Rajagopal, T. Shimasaki, P. E. Dotti, K. M. Fujiwara, K. Singh, Z. A. Geiger, and D. M. Weld, Nat. Commun. **9**, 2065 (2018).
[15] A. Bohrdt, D. Greif, E. Demler, M. Knap, and F. Grusdt, Phys. Rev. B **97**, 125117 (2018).
[16] J. T. Stewart, J. P. Gaebler, and D. S. Jin, Nature **454**, 744 (2008).
[17] L. Miaja-Avila, G. C. ONeil, Y. I. Joe, B. K. Alpert, N. H. Damrauer, W. B. Doriese, S. M. Fatur, J. W. Fowler, G. C. Hilton, R. Jimenez, et al., Phys. Rev. X **6**, 031047 (2016).
[18] D. Fausti, R. I. Tobey, N. Dean, S. Kaiser, A. Dienst, M. C. Hoffmann, S. Pyon, T. Takayama, H. Takagi, and A. Cavalleri, Science **331**, 189 (2011).
[19] H. Matsuzaki, H. Nishioka, H. Uemura, A. Sawa, S. Sota, T. Tohyama, and H. Okamoto, Phys. Rev. B **91**, 081114(R) (2015).
[20] Y. M. Sheu, S. A. Trugman, L. Yan, C. P. Chuu, Z. Bi, Q. X. Jia, A. J. Taylor, and R. P. Prasankumar, Phys. Rev. B **88**, 020101(R) (2013).
[21] M. Gandolfi, G. L. Celardo, F. Borgonovi, G. Ferrini, A. Avella, F. Banfi, and C. Giannetti, Phys. Scr. **92**, 034004 (2017).
[22] S. Hellmann, T. Rohwer, M. Kalläne, K. Hanff, C. Sohrt, A. Stange, A. Carr, M. M. Murnane, H. C. Kapteyn, L. Kipp, et al., Nat. Commun. **3**, 1069 (2012).
[23] H. Yamakawa, T. Miyamoto, T. Morimoto, T. Terashige, H. Yada, N. Kida, M. Suda, H. M. Yamamoto, R. Kato, K. Miyagawa, et al., Nat. Mater. **16**, 1100 (2017).
[24] H. Gomi, T. Kawatani, T. J. Inagaki, and A. Takahashi, J. Phys. Soc. Jpn. **83**, 094714 (2014).
[25] J. Weisshaupt, V. Juvé, M. Holtz, S. Ku, M. Woerner, T. Elsaesser, S. Ališauskas, A. Pugzlys, and A. Baltuška, Nat. Photon. **8**, 927 (2014).
[26] D. Popmintchev, B. R. Galloway, M.-C. Chen, F. Dollar, C. A. Mancuso, A. Hankla, L. Miaja-Avila, G. ONeil, J. M. Shaw, G. Fan, et al., Phys. Rev. Lett. **120**, 093002 (2018).
[27] G. Berner, M. Sing, H. Fujiwara, A. Yasui, Y. Saitoh, A. Yamasaki, Y. Nishitani, A. Sekiyama, N. Pavlenko, T. Kopp, et al., Phys. Rev. Lett. **110**, 247601 (2013).
[28] M. Guarise, B. D. Piazza, H. Berger, E. Giannini, T. Schmitt, H. M. Rønnow, G. A. Sawatzky, J. van den Brink, D. Altenfeld, I. Eremin, et al., Nat. Commun. **5**, 5760 (2014).
[29] F. Y. Bruno, S. Valencia, R. Abrudan, Y. Dumont, C. Carrétéro, M. Bibes, and A. Barthélémy, Appl. Phys. Lett. **104**, 021920 (2014).
[30] B. Torriss, J. Margot, and M. Chaker, Sci. Rep. **7**, 40915 (2017).
[31] D. Preziosi, L. Lopez-Mir, X. Li, T. Cornelissen, J. H. Lee, F. Trier, K. Bouzehouane, S. Valencia, A. Gloter, A. Barthélémy, et al., Nano Lett. **18**, 2226 (2018).
[32] C. Giannetti, M. Capone, D. Fausti, M. Fabrizio, F. Parmigiani, and D. Mihailovic, Adv. Phys. **65**, 58 (2016).
[33] M. Ligges, I. Avigo, D. Golež, H. U. R. Strand, Y. Beyazit, K. Hanff, F. Diekmann, L. Stojchevska, M. Kalläne, P. Zhou, et al., Phys. Rev. Lett. **120**, 166401 (2018).
[34] P. J. W. Weijs, M. T. Czyżyk, J. F. van Acker, W. Speier, J. B. Goedkoop, H. van Leuken, H. J. M. Hendrix, R. A. de Groot, G. van der Laan, K. H. J. Buschow, et al., Phys. Rev. B **41**, 11899 (1990).
[35] V. Mauchamp, M. Jaouen, and P. Schattschneider, Phys. Rev. B **79**, 235106 (2009).
[36] C. Suzuki, T. Nishi, M. Nakada, M. Akabori, M. Hirata, and Y. Kaji, J. Phys. Chem. Solids **73**, 209 (2012).
[37] J. C. Fuggle and N. Mårtensson, J. Electron. Spectrosc. Relat. Phenom. **21**, 275 (1980).
[38] See Supplemental Material for the derivation of effective single band model, the photoemission spectroscopy, and the NEXAS for different frequency and systems away from half filling, which includes Refs. [61-74].
[39] A. Hariki, T. Uozumi, and J. Kuneš, Phys. Rev. B **96**, 045111 (2017).
[40] S. R. White, Phys. Rev. Lett. **69**, 2863 (1992).
[41] U. Schollwöck, Ann. Physics **326**, 96 (2011).
[42] P. Silvi, D. Rossini, R. Fazio, G. E. SANTORO, and V. Giovannetti, Int. J. Mod. Phys. B **27**, 1345029 (2012).
[43] G. Vidal, Phys. Rev. Lett. **91**, 147902 (2003).
[44] G. Vidal, Phys. Rev. Lett. **93**, 040502 (2004).
[45] A. E. Feiguin and S. R. White, Phys. Rev. B **72**, 020404(R) (2005).
[46] A. J. Daley, C. Kollath, U. Schollwöck, and G. Vidal, J. Stat. Mech. **2004**, P04005 (2004).
[47] I. P. McCulloch, J. Stat. Mech. p. P10014 (2007).
[48] C.-Y. Lai, J.-T. Hung, C.-Y. Mou, and P. Chen, Phys. Rev. B **77**, 205419 (2008).
[49] C.-Y. Lai and C.-C. Chien, Sci. Rep. **6**, 37256 (2016).
[50] E. H. Lieb and F. Y. Wu, Phys. Rev. Lett. **20**, 1445 (1968).
[51] E. H. Lieb and F. Y. Wu, Physica A Stat . Mech. Appl. **321**, 1 (2003).
[52] P. A. van Aken and B. Liebscher, Phys Chem Min **29**, 188 (2002).
[53] H. Tan, J. Verbeeck, A. Abakumov, and G. Van Tendeloo, Ultramicroscopy **116**, 24 (2012).
[54] A. V. Balatsky, I. Vekhter, and J.-X. Zhu, Rev. Mod. Phys. **78**, 373 (2006).
[55] T. E. Kidd, T. Valla, P. D. Johnson, K. W. Kim, G. D. Gu, and C. C. Homes, Phys. Rev. B **77**, 054503 (2008).
[56] A. Keren, L. P. Le, G. M. Luke, B. J. Sternlieb, W. D. Wu, Y. J. Uemura, S. Tajima, and S. Uchida, Phys. Rev. B **48**, 12926 (1993).
[57] N. Motoyama, H. Eisaki, and S. Uchida, Phys. Rev. Lett. **76**, 3212 (1996).
[58] M. Hase, I. Terasaki, and K. Uchinokura, Phys. Rev. Lett. **70**, 3651 (1993).
[59] B. J. Kim, H. Koh, E. Rotenberg, S.-J. Oh, H. Eisaki, N. Motoyama, S. Uchida, T. Tohyama, S. Maekawa, Z.-X. Shen, et al., Nat. Phys. **2**, 397 (2006).
[60] Y. J. Kao, Y. D. Hsieh, and P. Chen, J. Phys. Conf. Ser. **640**, 012040 (2015).
[61] N. A., U. Kumar, N. Kaushal, G. Alvarez, E. Dagotto, and

S. Johnston, Sci. Rep. **8**, 11080 (2018).
[62] D. Benjamin, I. Klich, and E. Demler, Phys. Rev. Lett. **112**, 247002 (2014).
[63] C. Jia, K. Wohlfeld, Y. Wang, B. Moritz, and T. P. Devereaux, Phys. Rev. X **6**, 021020 (2016).
[64] M. Kanász-Nagy, Y. Shi, I. Klich, and E. A. Demler, Phys. Rev. B **94**, 165127 (2016).
[65] E. Jeckelmann, Phys. Rev. B **66**, 045114 (2002).
[66] T. D. Kühner and S. R. White, Phys. Rev. B **60**, 335 (1999).
[67] K. A. Hallberg, Adv. Phys. **55**, 477 (2006).
[68] H. Benthien, F. Gebhard, and E. Jeckelmann, Phys. Rev. Lett. **92**, 256401 (2004).
[69] M. Ganahl, M. Aichhorn, H. G. Evertz, P. Thunström, K. Held, and F. Verstraete, Phys. Rev. B **92**, 155132 (2015).
[70] F. Carbone, D.-S. Yang, E. Giannini, and A. H. Zewail, Proc. Natl. Acad. Sci. **105**, 20161 (2008).
[71] C. Kim, Z.-X. Shen, N. Motoyama, H. Eisaki, S. Uchida, T. Tohyama, and S. Maekawa, Phys. Rev. B **56**, 15589 (1997).
[72] C. Kim, A. Y. Matsuura, Z.-X. Shen, N. Motoyama, H. Eisaki, S. Uchida, T. Tohyama, and S. Maekawa, Phys. Rev. Lett. **77**, 4054 (1996).
[73] G. Barcza, O. Legeza, F. Gebhard, and R. M. Noack, Phys. Rev. B **81**, 045103 (2010).
[74] G. Barcza, W. Barford, F. Gebhard, and O. Legeza, Phys. Rev. B **87**, 245116 (2013).